2002-05-01

In-Plane Linear-Displacement Bistable Microrelay

Troy Gomm

Larry L. Howell
lhowell@byu.edu

Richard H. Selfridge
selfridge@ee.byu.edu

IN-PLANE LINEAR-DISPLACEMENT BISTABLE MICRORELAY

Troy Gomm
Ford Motor Company
2289 Abbey Ct.
Canton, MI 48188
tgomm@ford.com

Larry L. Howell
Mechanical Engineering
Department
Brigham Young University
Provo, UT 84602
lhowell@et.byu.edu

Richard H. Selfridge
Electrical & Computer
Engineering Department
Brigham Young University
Provo, UT 84602
selfridg@ee.byu.edu

ABSTRACT

This paper investigates the Linear Displacement Bistable Mechanism (LDBM) for use in microrelays. The LDBM, thermal actuators, and contacts are integrated to demonstrate a relay design. The performance of the relay is characterized using relay performance metrics, including size (1.92 mm^2), contact force (23.4 μN), switching time (340 μs), breakdown voltage (> 475 V), and isolation (> 235 V). The actuation voltage and current are 11 V and 85 mA, respectively. AC characteristics, including contact-to-contact crosstalk and AC isolation are also measured. The testing results demonstrate that it is feasible to use the LDBM as a microrelay and that it has potential for use in future applications.

INTRODUCTION

MEMS relays have many possible applications and have the potential to reduce the size, weight, power consumption, and cost of products in which they are used. In applications such as telecommunications switching in base stations and hand-held devices, one type of relay that will be valuable is a bistable microrelay – a microrelay that only requires power to switch from one state to another. Bistable microrelays offer potential advantages over current microswitches, such as field effect transistors, in that they require zero power consumption to remain in the switched position and their motion produces large gaps between contacts – which is desirable for high voltage switching and high breakdown voltages.

One difficulty for many bistable micromechanisms is that they require the use of large-clearance pin joints that can cause reliability problems for the mechanism. For example, in high frequency applications, moving linkages cause impacts in the pin joint that cause the joint to quickly fill with debris [1] - leading to wear out failure.

Recent research in compliant mechanisms application has yielded micro-scale compliant structures capable of bistable behavior [2, 3]. These mechanisms have the potential to solve several problems associated with current MEMS relays. Specifically, compliant structures could replace mechanisms that rely solely on pin joints to achieve their motion. This would allow microrelays to be fabricated more easily and operate more reliably.

This paper shows the feasibility and methods for creating Linear Displacement Bistable Mechanisms (LDBM), compliant bistable mechanisms, as microrelays. This is done by demonstrating the system integration of the compliant bistable micromechanism design and an actuator to create relays, and characterizing them using common relay performance metrics.

BACKGROUND

There are two main categories to differentiate microrelay operation: i) latching vs. non-latching and ii) normally open vs. normally closed. Latching relays (Form P) are those that consume power to switch positions (i.e. from "off" to "on") while non-latching relays consume power both to switch and to remain in the switched position. Non-latching relays may be designated as either normally open – when no power is being consumed, the contacts are open (Form A), or normally closed – when no power is being consumed, the contacts are closed (Form B).

Nearly all of the microrelays developed thus far are non-latching and normally open [4, 5, 6, 7, 8, 9, 10]. There are some latching relays [11] but these generally have required a complex control signal and mechanical design to achieve their latching ability. Mercury microdrops have been demonstrated as latching-type microrelays [12].

Another important feature of relays is their contacts. Many different types of contacts have been used in conjunction with MEMS relays. However, there are two basic attributes that may be used to categorize relay contacts: their material and their motion. Ideal contact materials provide a low electrical resistance and a high mechanical resistance to wear. The ideal motion is one that removes oxide layers, results in a high contact area, and is robust to wear and other changes.

Gold is the primary material used to fabricate current MEMS relay contacts. This is due to its high electrical conductivity, softness, and availability in commercial processes [13]. Other contact materials have also been used including nickel to gold [7], nickel-iron to gold [6], and mercury [12, 14].

There are two main types of contact configurations – as described by their contact motion – horizontal and vertical. Vertical motion contacts move out of plane to make contact and the con-

nection is made by the top or bottom surface of the contact. Horizontal contacts move in-plane and make the connection with the side of the contact.

Contact materials used to achieve low contact resistance are generally not good structural materials (gold for example) so the contact will often have a structural portion that has some layer or coating of contact material. Because of this, vertical motion contacts are used much more frequently due to the comparative ease of fabricating horizontal layers [4, 5, 6, 7, 8, 9]. Horizontal contacts are less common due to the difficulty of depositing contact material on the vertical walls that will make contact [13].

Another characteristic of relay motion concerns the number of stable equilibrium positions in its motion. An equilibrium position is a position in which the mechanism has no acceleration. Equilibrium positions of a mechanism occur where the derivative of a mechanism's potential energy equation equals zero. An equilibrium state is *unstable* if small disturbances cause the mechanism to deviate from its position and not return. If the mechanism returns to the equilibrium position after being disturbed, the position is a *stable* equilibrium position. If the mechanism is disturbed and stays in the disturbed position, it is in a *neutral* equilibrium.

A given equilibrium position can be found to be stable or unstable by taking the second derivative of the mechanism's potential energy equation. If the second derivative is negative at the equilibrium position, it is an unstable equilibrium. If it is positive, the equilibrium position is stable. Figure 1 shows the common "Ball on a Hill" analogy for equilibrium positions. A bistable mechanism has two stable equilibrium positions. One advantage of using bistable mechanisms in relays is that the two stable positions correspond to "on" and "off" states. Power is only required to transition between the states, not to maintain a state. The Linear Displacement Bistable Mechanism (LDBM) is a bistable mechanism, and is described next.
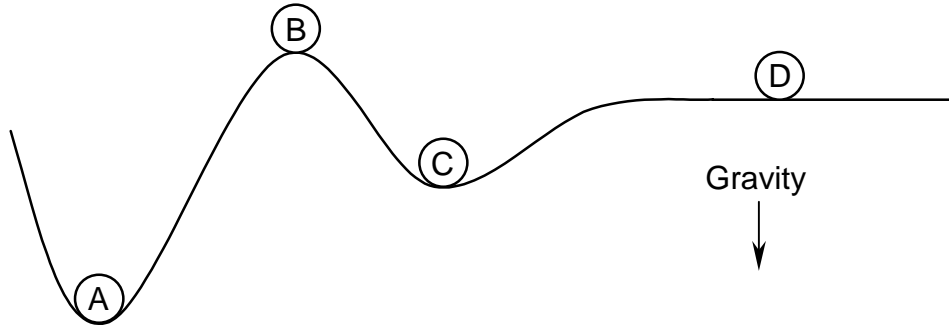
Figure 1   Ball-on-hill analogy: balls A and C are in stable equilibrium positions, ball B is in an unstable equilibrium position, and ball D is in a neutral equilibrium position.
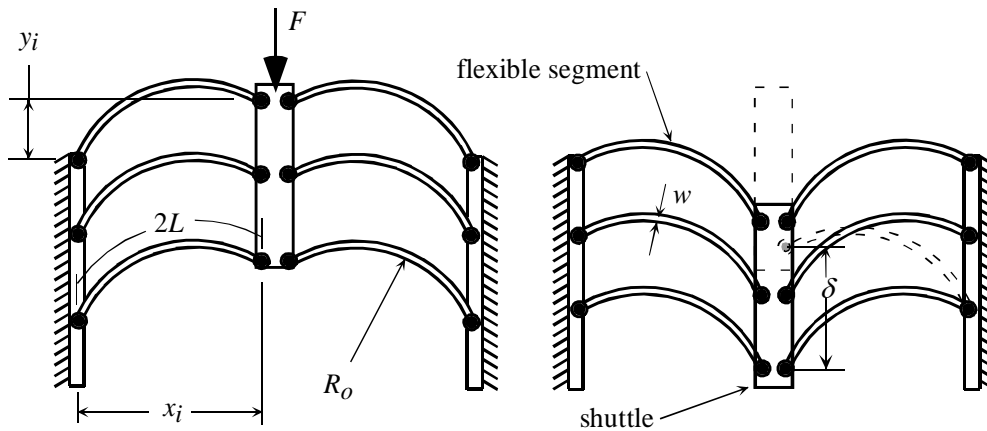

Figure 2   Linear Displacement Bistable Mechanism (LDBM).

LINEAR DISPLACEMENT BISTABLE MECHANISMS

A compliant mechanism is a device that derives some (partially compliant) or all (fully compliant) of its motion from the deflection of its members [15]. Several compliant microbistable mechanisms have been developed [2, 16, 18]. The performance of one of these, the Linear Displacement Bistable Mechanism (LDBM) [3], is the subject of this work.

The LDBM is composed of a central slider with an array of functionally binary pinned-pinned (FBPP) segments ("legs") on each side, as illustrated in Figure 2. and Figure 3. Because
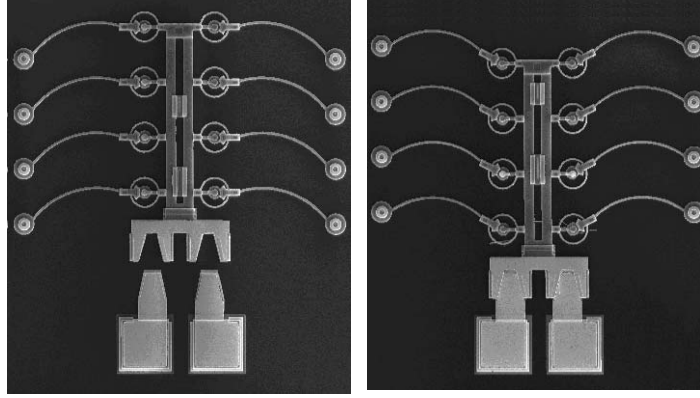
Figure 3   A scanning electron microscope photo of an LDBM shown in both positions.

the segments have pin joints on each side, they can only support loads acting in-line with the pins. The segments cannot support any other loads including moments. Because of this, the segments act as linear springs with non-linear force-deflection relationships. By fabricating the FBPP segments at an angle to the slider, the device achieves its bistable behavior.

The potential energy curve and, therefore, the equilibrium positions of the LDBM can be found using the pseudo-rigid-body model [19]. The pseudo-rigid-body model is a method of modeling compliant mechanisms by accurately approximating flexible segments with rigid segments and torsional springs. The potential energy, V, for a half-segment may be calculated as

$$V = \frac{1}{2}K(\Theta - \Theta_i)^2 \tag{1}$$

where K is the pseudo-rigid-body spring constant

$$K = \rho K_\Theta \frac{EI}{L} \tag{2}$$

and Θ is the pseudo-rigid-body angle which is related to the shuttle deflection, δ, as

$$\Theta = \text{asin}\left(\frac{\sqrt{x_i^2 + (y_i - \delta)^2} - 2(1 - \gamma)L}{2\rho L}\right) \tag{3}$$
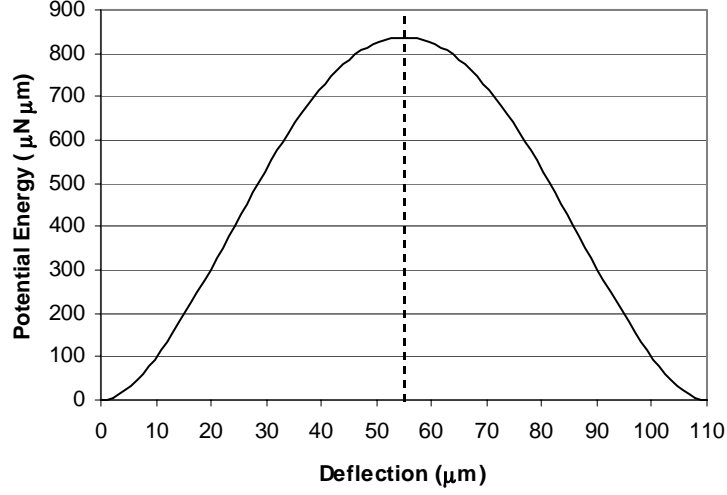
and

Figure 4   Potential energy curve for the LDBM with parameters listed in Table 1.

$$\rho = \sqrt{\left[\frac{R_o}{L}\sin\left(\frac{L}{R_o}\right) - (1-\gamma)\right]^2 + \left[\frac{R_o}{L}\left(1 - \cos\frac{L}{R_o}\right)\right]^2} \qquad (4)$$

where y_i is the pin-to-pin distance in the δ direction, x_i is the pin-to-pin distance in the direction perpendicular to δ, R_o is the initial radius of curvature of the flexible segment, γ is the character-istic radius factor, K_Θ is the stiffness coefficient, E is Young's modulus, and L half the length of the flexible segment. Θ_i is the initial pseudo-rigid-body angle and is found using equation (3) with $\delta = 0$. I is the area moment of inertia and is equal to $I = wt^2/12$ where w is the segment in-plane width and t is the out-of-plane thickness. More detail on the above equations can be found in [20] and the variables are illustrated in Figure 2.

The potential energy curve for the LDBM is shown in Figure 4. The mechanism geometry and the pseudo-rigid-body parameters necessary to generate the potential energy curve are shown in Table 1. The mechanism was fabricated using the MUMPs [21] surface micromachining pro-cess and then tested to characterize their behavior as relays, as described in the following section.

RELAY PERFORMANCE

Performance metrics can be used to characterize a relay's behavior. The contact force, switching time, contact-to-contact crosstalk, AC isolation, breakdown voltage, and isolation were measured for the LDBM. The results for each of these metrics are reported next.

Contact Force

High contact forces can help lower contact resistance and reduce bounce on closing. The factors that lead to higher contact forces also lead to faster switching times. It is very difficult to measure contact force at the micro level. Analytical predictions of contact force were combined with the results of contact-force measurements to characterize the behavior of the LDBM relays.

The force predictions were made by differentiating the potential energy equation (1) with respect to deflection (Figure 5). This results in a maximum predicted contact force for the LDBM

Table 1: Variable values for LDBM potential energy curve calculations.

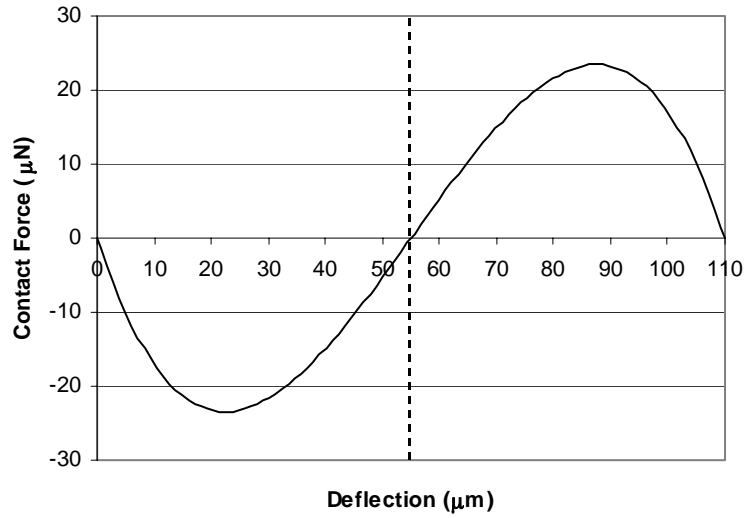| Variable	Value	Unit
R_o	144	μm
L	122.94	μm
γ	0.7857	
ρ	0.7799	
K_Θ	2.644	
E	1.69E+11	Pa
w	4	μm
t	2	μm
I	10.667	μm^4
K	30236	μN*μm
Θ_i	0.5309	Radians
x_i	210	μm
y_i	55	μm
Segments per side	3	

Figure 5   Predicted contact force as a function of shuttle deflection for the LDBM with parameter values listed in Table 2.

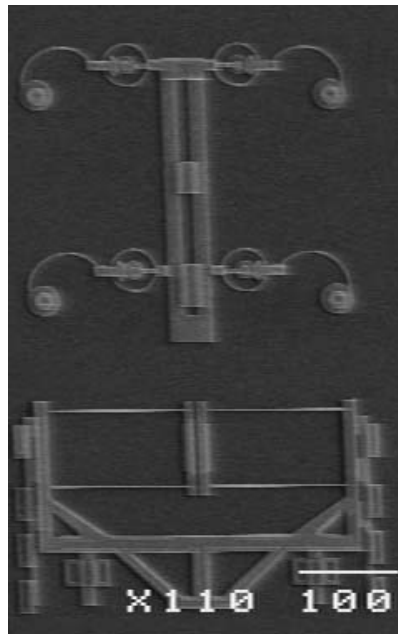Figure 6   Setup of contact force tests.

of 23.4 μN at 88 μm.

To allow for contact force measurement, a force tester [22] was placed next to the mechanisms (Figure 6). To measure the contact force, each mechanism was switched from its fabricated

position to its second stable equilibrium position. The force testers were then manually translated toward the mechanism. When the mechanism was in contact with the force tester, the tester was used to push the mechanism back through its unstable equilibrium position to snap back to its original position. The force-tester deflections were measured optically and the reaction force was then determined. The variable values used to calculate the contact force curve are listed in Table 2.

The measured forces follow the same trend as the predicted forces but are significantly higher. This is a measure of the stiction at the location of the device on the die used for the test, and had an average value of 365 μN. This value is higher than the maximum predicted reaction force, and has a nontrivial effect on the motion. Stiction makes verification of the contact force predictions difficult, but more importantly, it reduces the amount of force imparted to the contact. This is being addressed in future designs by eliminating the pin joints and suspending the mechanism above the substrate, such as described in [17] and [18].

Table 2: Variable values for LDBM contact force calculations.

Variable	Value	Unit
R_o	53	μm
L	81.59	μm
γ	0.7857	
ρ	0.7583	
K_Θ	2.8496	
E	1.69E+11	Pa
w	4	μm
t	2	μm
I	10.667	μm^4
K	47738	μN*μm
Θ_i	0.9788	Radians
x_i	100	μm
y_i	35	μm
Segments per side	2	

The contact resistance was measured from bond pad to bond pad to be 49.2 Ω. This resistance could be decreased by improving the contact force (such as reducing stiction effects) and by investigating improved contact surfaces for in-plane relays.

Switching Time

Switching time is a critical relay performance parameter. Shorter switching times mean higher frequency ranges and therefore expanded application possibilities. The full LDBM relay used for these tests includes the mechanism, contacts, and actuators.

To measure the switching time, the actuation voltage and the contact voltage were plotted simultaneously on a digital oscilloscope. The time separation of the two voltage steps indicated the switching time. The contact voltage that was measured was the voltage between one contact and the common ground (the same ground used for the actuation circuit).

The switching time of the LDBM was measured to be 340 μs with a standard deviation of 20 μs. A current pulse of 85 mA was used to achieve contact and measure the switching time. This is well within the range of the switching times of current microrelays. The geometry of the LDBM used is the same as that given in Table 1 with 2 legs per side rather than 3.

The actuator design plays as important a role in determining switching time as the mechanism design. This is because the contacts are fairly close to the unstable equilibrium positions. The mechanisms are therefore pushed all the way to contact by the actuators. The power used to actuate the mechanisms could be reduced so that the mechanisms would be pushed just past their unstable positions, but this would also increase the switching time.
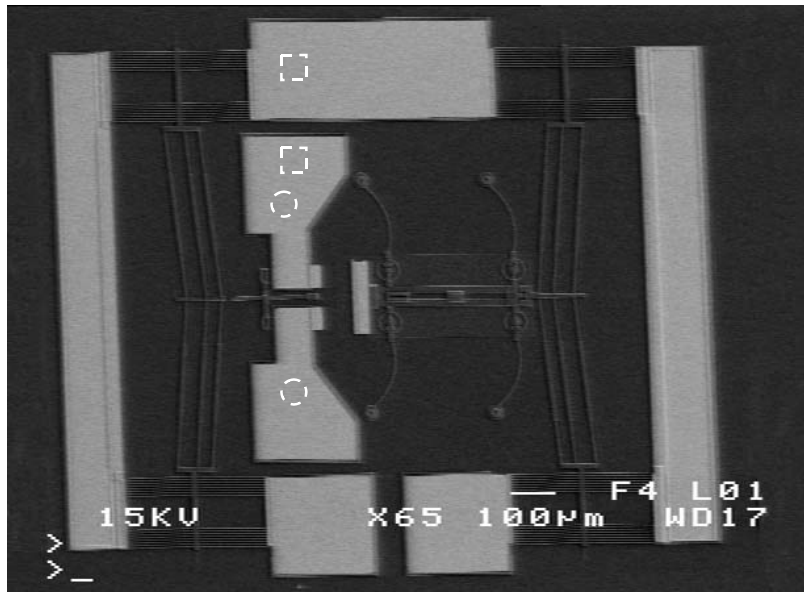
Figure 7   Linear Displacement Bistable Mechanism relay used for AV characteristics test. Circles represent probe locations for the contact-to-contact crosstalk test and squares represent probe locations for the AC isolation test.

AC Characteristics

AC characteristics of current microrelays are generally not documented because most microrelays are designed for DC or low frequency signal use. The LDBM relay is also intended for DC or low frequency use. However, there are two AC signal characteristics that are of interest: contact-to-contact crosstalk and AC isolation. Contact-to-contact crosstalk refers to the ratio of the output signal to the input signal, where the output signal is induced across the open contact. AC isolation is the ratio of the signal induced in the actuation circuit (by the input signal) to the input signal.

The contact-to-contact crosstalk and AC isolation are dependent upon contact design and actuation circuit layout rather than the design of the mechanism used. Figure 7 show the relays used for the AC characteristics tests as well as the probe locations for each of the tests.
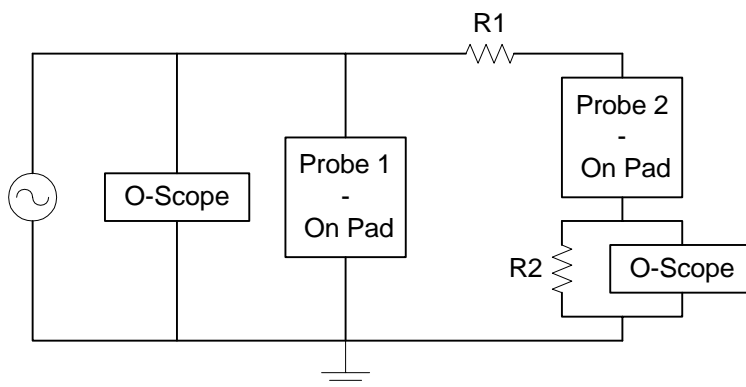
Figure 8   Electrical diagram of experimental setup. R1 represents the resistance of the air gap in parallel with the nitride layer and substrate. R2 is a 1 kΩ resistor.

For both the contact-to-contact crosstalk and the AC isolation tests, a function generator was used to apply AC sine wave signals from 1 Hz to 1 MHz. All signals (applied and measured) shared a common ground. A digital oscilloscope was used to measure the amplitude of both the input signal and the induced signal. For each measurement, the oscilloscope averaged 8 samples of several periods.

In order to differentiate between signals induced on-chip and signals induced by the setup of the experiment (ex: signal wire or probe-to-probe crosstalk), the probe closest (electrically) to ground was lifted off the die and the induced signal was measured. The probe locations for the tests are shown in Figure 7, an electrical diagram of the experimental setup is shown in Figure 8.

Contact-to-Contact Crosstalk - The results of the contact-to-contact crosstalk measurements are shown in Figure 9. The horizontal axis is frequency (on a log scale) and the vertical axis is the ratio of the induced signal amplitude (in volts) to the input signal amplitude (also in volts). It can be seen from the graph that the LDBM relay crosstalk becomes measurable at around 10 kHz. An interesting feature of the LDBM graph is the large amount of system noise measured at 10 kHz.
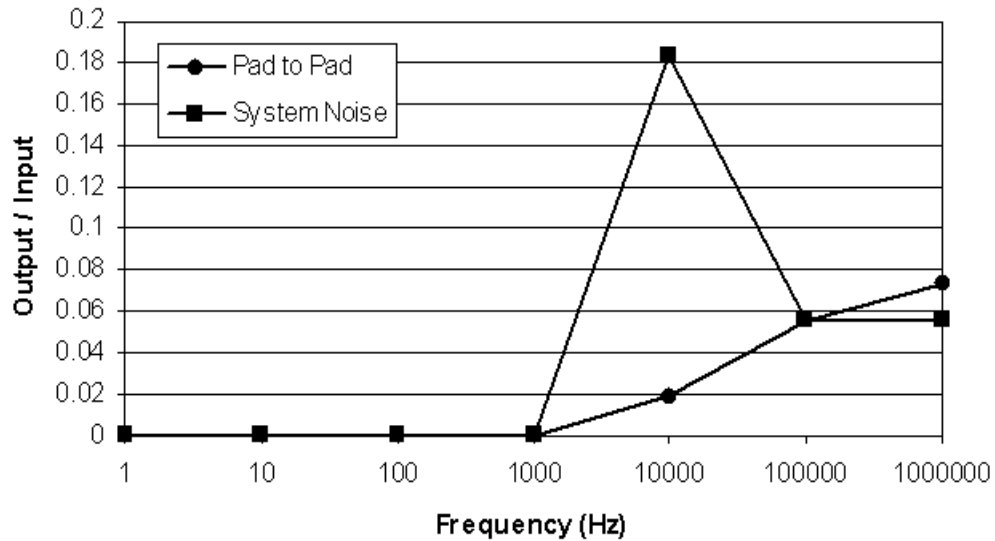
Figure 9   Contact-to-contact crosstalk for the LDBM relay.

This spike was measured several times and is not simply a statistical outlier. The exact cause of this large value is not known, but may be due to system resonance.

AC Isolation- The results of the AC isolation measurements for the LDBM relay are shown in Figure 10. The axes are the same as those for Figure 9. It can be seen that the AC Isolation begins to decrease at around 10 kHz. As in the contact-to-contact crosstalk graph, a large, unexplained spike in system noise was repeatedly measured at 10 kHz.

Considering that the relay was designed for DC to low frequency use, the relay performed well. From the AC characteristics tests it can be seen that AC signals do not adversely affect relay performance, in terms of contact-to-contact crosstalk and AC isolation, until around 10 kHz. This suggests that these relays are suitable for low-frequency applications, but the current configuration would be unacceptable for high-frequency applications.
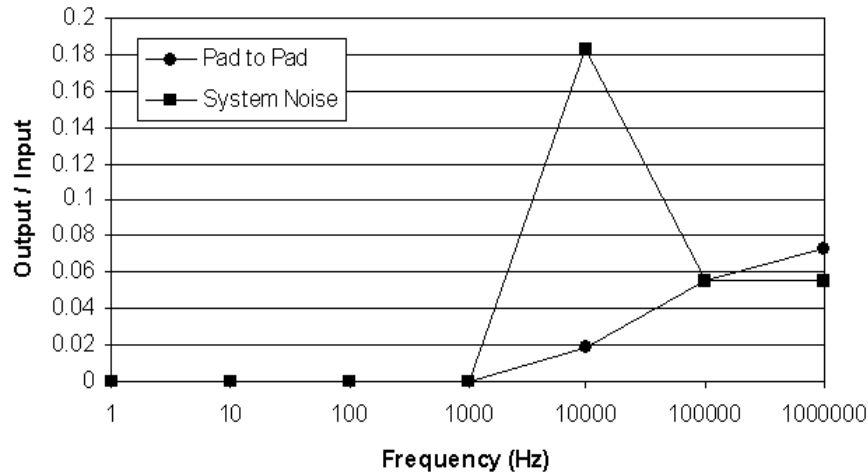
Figure 10   AC isolation measurements for the LDBM relay.

The factors that are thought to affect both the contact-to-contact crosstalk and the AC isolation of the relays include pad / actuation current path separation, nitride thickness, relative current line orientation (parallel vs. perpendicular), current line / contact pad areas, and dielectric strength between pads. These are considered to be the important factors because they are the main contributors to resistance and capacitance between the contacts and between the contacts and the actuation circuits. In order to optimize the AC performance of the relays, future research should begin with a study to quantitatively characterize the contacts and actuation circuits as functions of these factors. Another avenue for further research would be to test the relays with equipment designed to reduce the system noise and isolate the AC characteristics of the relays. Some factors that may contribute to system noise include wire shielding, wire length, and probe separation.

Voltage Characteristics

The voltage characteristics of a relay are important performance parameters for determining its potential applications. The higher the voltage the relay can withstand, the broader the potential applications.
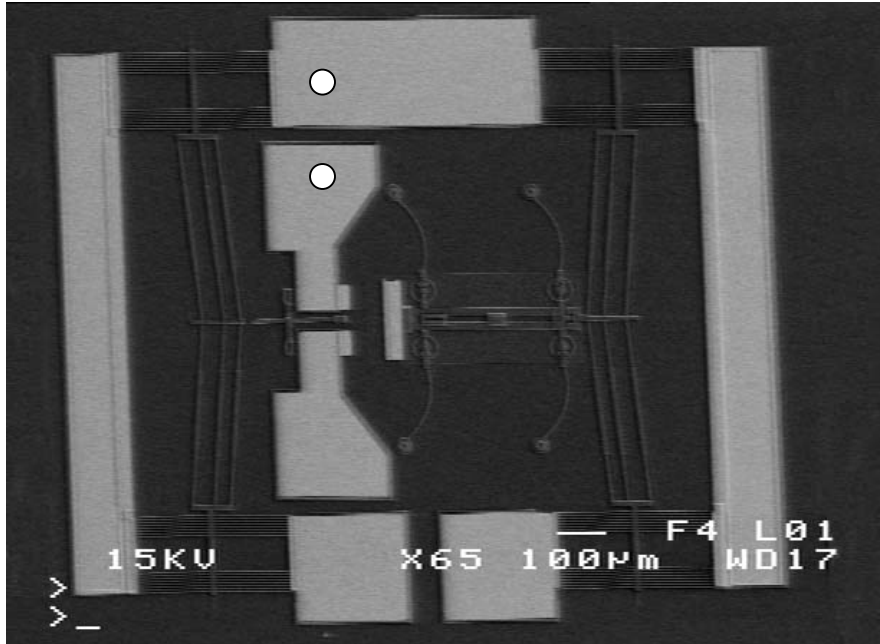
Figure 11   Relay used for voltage characteristics tests. White dots indicate probe positions for the isolation tests.

The physical layout of the voltage experiment was the same as that of the AC characteristics experiments and the switching time experiments. The relay shown in Figure 11 and two small contact pads (each 92 μm by 92 μm separated by a 2 μm gap) were used for the tests. The small pads were included in the test to determine the effect of very small separation distances. The breakdown voltage characteristics are dependent upon pad design and current line layout rather than on the mechanism used to move the contact.

To measure the open circuit contact-to-contact breakdown voltage, a high voltage power supply as used. The voltage was applied to the two contact pads with the relay in the open position. The current limit on the power supply was set to 0.1 mA and the voltage was slowly increased until the current limit tripped.
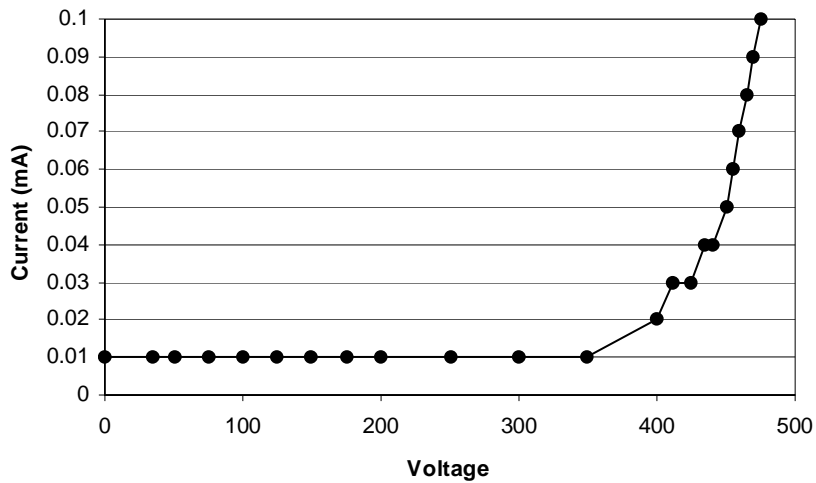
Figure 12 Results of the breakdown voltage test.

Breakdown Voltage - The results of the breakdown voltage test on the relay are summarized in Figure 12. It should be noted that for the equipment used, 0.01 mA is the lowest current measurement that can be displayed so should be considered to be effectively zero current flow. From the figure, it can be seen that current begins to leak at around 400 V. The pad separation for this test was 33 μm.

The tests using smaller pads were more dramatic. Because of the small separation, the pads experience dielectric breakdown rather than current leakage. The current was effectively zero until the point of breakdown, so a plot of applied voltage versus current is not included. The breakdown voltage was measured twice (with different sets of pads) and found to be 350 V and 360 V (see Figure 13).

Isolation- The results of the isolation test, along with a comparison to the breakdown voltage test, are summarized in Figure 14. The location of the isolation measurement is shown on Figure 11. It can be seen from the graph that current begins to leak at around 200 V. This lower voltage can be
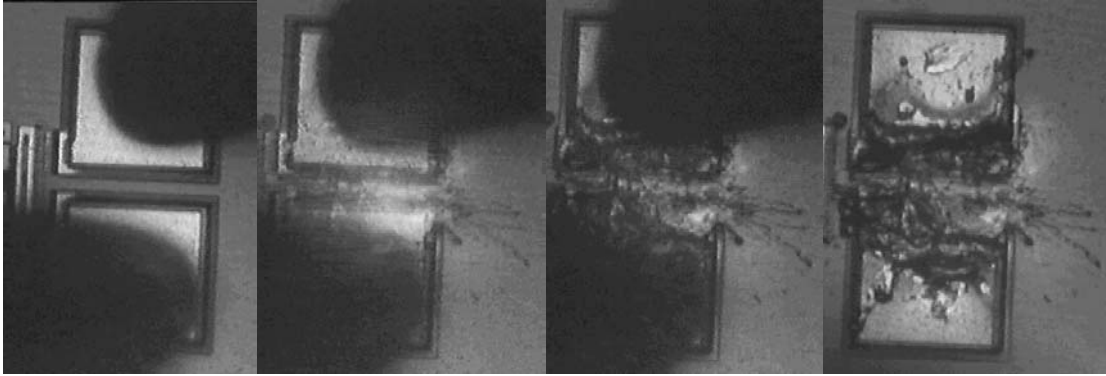
Figure 13   Steps of the breakdown process captured on video.
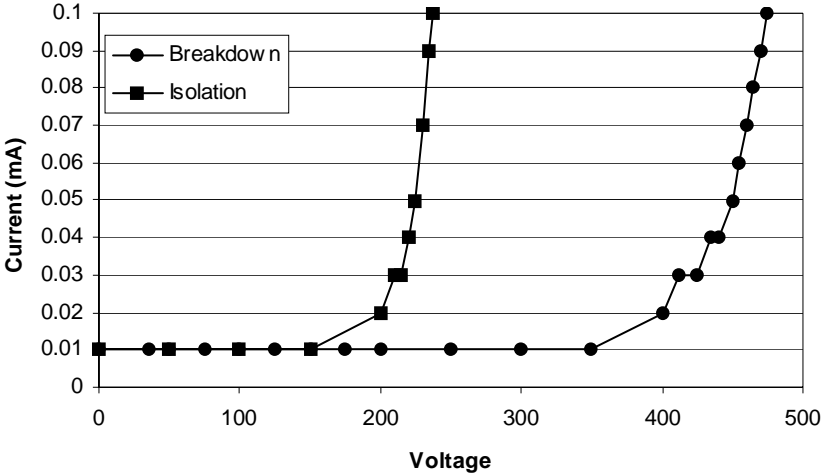
Figure 14   Results of the isolation test.

explained by the lower separation (25 μm for the isolation test as opposed to 33 μm for the break-

down test) and the large size of the pad on the actuation circuit.

The relay layouts used in this research perform well in terms of breakdown voltage. The

400 V breakdown characteristic is on the upper end of the range of current microrelays (Table 3).

This performance characteristic could be easily improved by increasing the separation between

the contact pads. The tests also show that attempts to decrease the pad separation (perhaps to

increase component density) could result in catastrophic failure (Figure 13).

The isolation measured for this relay layout is quite low. This performance characteristic could be improved by designing an actuation current path separated by a greater distance from the contact pads. It is recommended that future attempts to optimize the relay design (in terms of the trade-off between breakdown voltage, isolation, and component density) include a study to quantify the effects of pad size and separation.

CONCLUSION

This paper shows the feasibility and method of using LDBM's as microrelays. Existing mechanisms and actuators were integrated into a coherent switching system and the performance of the relays was characterized. A summary of the performance of the LDBM relays compared to that of the high and low values of other microrelays is given in Table 3. The values reported in the table represent the extreme high and low for any relay for each given parameter and does not represent a given relay. Table 4 compares the performance of three representative current microrelays [5, 6, 11] with those characterized in this paper. The relay in [6] has also been reported

Table 3: Comparison of relay performance parameters.

Attribute	Literature High		Literature Low		LDBM Relay	
Actuation Current	600	mA	50	nA	85	mA
Actuation Voltage	150	V	0.53	V	11	V
Actuation Power	320	mW	1	μW	935	mW
Breakdown Voltage	> 400	V	> 3	V	> 475	V
Contact Force	500	μN	3	μN	23.4	μN
Contact Resistance	300	Ω	22.4	m Ω	49.2	Ω
Displacement	16	μm	0.5	μm	88	μm
Isolation (DC)	>1600	V		—	> 235	V
Size	2.E+06	μm^2	1E+04	μm^2	1.92E+6	μm^2
Switching Time	5	ms	2	μs	340	μs

to work as a normally closed device [23]. Values missing from the table represents values that were not reported in the literature.

The LDBM works well as a relay. It has good values of contact force, switching time, and breakdown voltage. The large deflections of the mechanism leads to high breakdown voltages and isolations. This should make them suitable for higher voltage applications – such as telecommunications components for which high breakdown voltages are required. The general relay design in this paper compares favorable with other microrelays. If a particular application were selected for the relay, it could be optimized to improve the parameters of interest for that application.

A drawback of the LDBM is that it uses pin joints that provide a mechanism for mechanical wear and can lead to wear out failure distribution. Fully compliant micro bistable mechanisms have been designed to eliminate this problem [2, 16, 17, 18].

Table 4: Comparison of performance parameters for selected relays.

Attribute	Taylor et al. 1998		Schiele et al. 1998		Sun et al. 1998		LDBM	
Actuation Type	Magnetic		Electrostatic		Thermal		Thermal	
Actuation Current	600	mA	50–70	nA			85	mA
Actuation Voltage	*0.53*	*V*	20–150	V			11	V
Actuation Power	320	mW	1–10.5	μW	10–12	mW	935	mW
Hold Power	320	mW	1–10.5	μW	0		0	
Breakdown Voltage	>10	V			> 400	V	> 475	V
Contact Force	>1	mN			21	μN	23.4	μN
Contact Resistance	22.4–38.6	mΩ	10–80	Ω	2.1–35.6	Ω	49.2	Ω
Displacement	10	μm	10	μm	16	μm	88	μm
Isolation (DC)	>1600	V					> 235	V
Size	2.08	mm^2	0.03–0.7	mm^2			1.92	mm^2
Switching Time	0.5–5	ms	2.6–33	μs	0.1–0.5	ms	340	μs

The power consumption during switching is quite high compared to other microrelays. However, there are two things to keep in mind when considering the power consumption. First, power consumption is a function of actuator design and can be changed by optimizing the actuators' power performance. Second, because the mechanisms are bistable, power usage is only required during switching and not to hold the switch in either the "on" or "off" positions. This feature should make the relays appealing for applications in which the "on" or "off" hold time is high – such as DSL line diagnostic equipment.

ACKNOWLEDGMENTS

LIST OF REFERENCES

[1]   Tanner, Danelle M., Miller, William M., Eaton, William P., Irwin, Lloyd W., Peterson, Ken A., Dugger, Michael T., Senft, Donna C., Smith, Norman F., Tangyunyong, Paiboon, and Miller, Samuel L., 1998, "The Effect of Frequency on the Lifetim e of a Surface Micromachined Microengine Driving a Load," *1998 IEEE International Reliability Physics Symposium Proceedings*, March 30 - April 2, 1998, pp. 26-35.

[2]   Jensen, B. D., Howell, L. L., Salmon, L. G., 1999, "Design of Two-Link, In-Plane, Bistable Compliant Micro-Mechanisms," *Journal of Mechanical Design*, Trans. ASME, Vol. 121, September 1999, pp. 416-423.

[3]   Baker, Michael S., Lyon, Scott, M., and Howell, Larry L., 2000, "A Linear Displacement Bistable Micromechanism," *Proceedings of the 2000 ASME Design Engineering Technical Conferences*, DETC2000/MECH-14117.

[4]   Yao, J. Jason and Chang, M. Frank, 1995, "A Surface Micromachined Miniature Switch for Telecommunications Applications with Signal Frequencies from DC up to 4 GHz," *The 8th International Conference on Solid-State Sensors, and Eurosensors IX*, Stockholm Sweden, June 15-29, 1995, pp. 384-387.

[5] Schiele, Ignaz, Huber, Jörg, Hillerich, Bernd, and Kozlowski, Frank, 1998, "Surface-Micromachined Electrostatic Microrelay," *Sensors and Actuators A: Physical*, A 66, 1988, pp. 345-354.

[6] Taylor, William P., Brand, Oliver, and Allen, Mark G., 1998, "Fully Integrated Magnetically Actuated Micromachined Relays," *IEEE Journal of Microelectromechanical Systems*, Vol. 7, No. 2, June 1998, pp. 181-191.

[7] Grétillat, M-A., Grétillat F., and de Rooij, N.F., 1999, "Micromechanical Relay with Electrostatic Actuation and Metallic Contacts," *Journal of Micromechanics and Microengineering*, 1999, pp. 324-331.

[8] Yao, Z. Jamie, Chen, Shea, Eshelman, Susan, Denniston, David, and Goldsmith, Chuck, 1999, "Micromachined Low-Loss Microwave Switches," *IEEE Journal of Microelectromechanical Systems*, Vol. 8, No. 2, June 1999, pp. 129-134.

[9] Zhou, Shifang, Sun, Xi-Qing, and Carr, William, 1999, "A Monolithic Variable Inductor Network Using Microrelays with Combined Thermal and Electrostatic Actuation," *Journal of Micromechanics and Microengineering, 9,* 1999, pp. 45-50.

[10] Petersen, K.E., 1979, "Micromechanical Membrane Switches on Silicon," *IBM Journal of Research and Development*, Vol. 23-4, pp. 376-385.

[11] Sun, Xi-Quing, Farmer, K. R., and Carr, W. N., 1998, "A Bistable Microrelay Based on Two-Segment Multimorph Cantilever Actuators," *IEEE: Proceedings of The Eleventh Annual International Workshop on Micro Electro Mechanical Systems*, 1998, pp. 154-159.

[12] Simon, Jonathan, Saffer, Scott, and Kim, Chang-Jin, 1997, "A Liquid-Filled Microrelay with a Moving Mercury Microdrop," *IEEE Journal of Microelectromechanical Systems*, Vol. 6, No. 3, September 1997, pp. 208-216.

[13] Kruglick, Ezekial J. J. and Pister, Kristofer S. J., 1999, "Lateral MEMS Microcontact Considerations," *IEEE Journal of Microelectromechanical Systems*, Vol. 8, No. 3, September 1999, pp. 264-271.

[14] Lee, Junghoong, and Kim, Chang-Jin, 2000, "Surface-Tension-Driven Microactuation Based on Continuous Electrowetting," *IEEE Journal of Microelectromechanical Systems*, Vol. 9, No. 2, June 2000, pp. 171-179.

[15] Howell, L. L., 2001, *Compliant Mechanisms*, John Wiley and Sons, New York, NY.

[16] Parkinson, Matthew B., Jensen, Brian D., and Roach, Gregory M., 2000, "Optimization-Based Design of a Fully Compliant Bistable Micromechanism," *Proceedings of the 2000 ASME Design Engineering Technical Conferences*, DETC2000/MECH-14119.

[17] Jensen, B.D., Parkinson, M.B., Kurabayashi, K., Howell, L.L., and Baker, M.S., "Design Optimization of a Fully-Compliant Bistable Micro-Mechanism," *Proceedings of the 2001*

ASME International Mechanical Engineering Congress and Exposition, Microelectrome-chanical Systems Subdivision, November 2001, IMECE2001/MEMS-23852.

[18]   Masters, N., 2001, "On a Self-Retracting Fully-Compliant In-Plane Linear Motion Small-Displacement Bistable Micromechanism for Low Power Switching Applications," M.S. Thesis, Brigham Young University, Provo, Utah.

[19]   Howell, L. L. and Midha, A., 1995, "Parametric Deflection Approximations for End-Loaded, Large-Deflection Beams in Compliant Mechanisms," *Journal of Mechanical Design*, Trans. ASME, Vol. 117, No. 1, pp. 156-165

[20]   Gomm, T., "Development of In-Plane Compliant Bistable Microrelays," M.S. Thesis, Brigham Young University, August 2001.

[21]   Koester, D.A., Mahadevan, R., Hardy, B., and Markus, K.W., 2001, *MUMPs™ Design Handbook*, Revision 6.0, Cronos Integrated Microsystems, Research Triangle Park, NC.

[22]   Wittwer, J.W., Gomm, T., Howell, L.L., 2002, "Surface Micromachined Force Gauges: Uncertainty and Reliability," *Journal of Micromechanics and Microengineering*, Vol. 12, No. 1, pp. 13-20.

[23]   Taylor, W.P., Schneider, M., Balets, H., and Allen, M.G., "Electroplated Soft Magnetic Materials for Microsensors and Microactuators," *Proceedings of Trasducers '97,* Chicago, IL, Vol 2., pp. 793-796.